



Natural Resources
Canada

Ressources naturelles
Canada



Preliminary results of detrital muscovite $^{40}\text{Ar}/^{39}\text{Ar}$ geochronology from the eastern Mackenzie Mountains and Mackenzie Plain, Northwest Territories

J. Powell and D.A. Schneider

**Geological Survey of Canada
Current Research 2013-18**

2013

**Geological Survey of Canada
Current Research 2013-18**



**Preliminary results of detrital muscovite
 $^{40}\text{Ar}/^{39}\text{Ar}$ geochronology from the eastern
Mackenzie Mountains and Mackenzie Plain,
Northwest Territories**

J. Powell and D.A. Schneider

2013

©Her Majesty the Queen in Right of Canada 2013

ISSN 1701-4387

Catalogue No. M44-2013/18E-PDF

ISBN 978-1-100-22494-7

doi:10.4095/292712

A copy of this publication is also available for reference in depository libraries across Canada through access to the Depository Services Program's Web site at <http://dsp-psd.pwgsc.gc.ca>

This publication is available for free download through GEOSCAN
<http://geoscan.ess.nrcan.gc.ca>

Recommended citation

Powell, J. and Schneider, D.A., 2013. Preliminary results of detrital muscovite $^{40}\text{Ar}/^{39}\text{Ar}$ geochronology from the eastern Mackenzie Mountains and Mackenzie Plain, Northwest Territories; Geological Survey of Canada, Current Research 2013-18, 16 p. doi:10.4095/292712

Critical review

D. Kellett

Authors

J. Powell (jpowe068@uottawa.ca)

D.A. Schneider (david.schneider@uottawa.ca)

Department of Earth Sciences

University of Ottawa

140 Louis Pasteur Private

Ottawa, Ontario

K1N 6N5

Correction date:

**All requests for permission to reproduce this work, in whole or in part, for purposes of commercial use, resale, or redistribution shall be addressed to: Earth Sciences Sector Copyright Information Officer, Room 622C, 615 Booth Street, Ottawa, Ontario K1A 0E9.
E-mail: ESSCopyright@NRCan.gc.ca**

Preliminary results of detrital muscovite $^{40}\text{Ar}/^{39}\text{Ar}$ geochronology from the eastern Mackenzie Mountains and Mackenzie Plain, Northwest Territories

J. Powell and D.A. Schneider

Powell, J. and Schneider, D.A., 2013. Preliminary results of detrital muscovite $^{40}\text{Ar}/^{39}\text{Ar}$ geochronology from the eastern Mackenzie Mountains and Mackenzie Plain, Northwest Territories; Geological Survey of Canada, Current Research 2013-18, 16 p. doi:10.4095/292712

Abstract: Single-grain detrital muscovite $^{40}\text{Ar}/^{39}\text{Ar}$ geochronology was performed on eight siliciclastic samples from the Mackenzie Mountains and Mackenzie Plain of the Northwest Territories. The rocks encompass two separate sample suites: the Neoproterozoic Mackenzie Mountains Supergroup and the Devonian Imperial Formation. A majority of the muscovite sample ages (1200–875 Ma) from the Neoproterozoic strata suggest derivation from a Grenvillian-aged source to the east. Detrital ages from individual samples serve to refine the poorly constrained stratigraphic ages for formations within the supergroup. Single-grain ages from the Imperial Formation range between 650–350 Ma, with a 425–400 Ma mode corresponding to the timing of collision between ancestral North America and a northern landmass throughout the Devonian. These new data allow re-evaluation of current understanding of both the post-Grenvillian and pre-Ellesmerian source to sink pathways for siliciclastic strata of the Mackenzie River corridor.

Résumé : Une géochronologie $^{40}\text{Ar}/^{39}\text{Ar}$ sur des grains individuels de muscovite détritique a été effectuée sur huit échantillons de roches silicoclastiques provenant des monts Mackenzie et de la plaine du Mackenzie dans les Territoires du Nord-Ouest. Les roches appartiennent à deux suites d'échantillons distinctes : le Supergroupe de Mackenzie Mountains du Néoprotérozoïque et la Formation d'Imperial du Dévonien. Une majorité des âges d'échantillons de muscovite (1200-875 Ma) provenant des strates du Néoprotérozoïque indique comme origine une source d'âge grenvillien à l'est. Les âges de minéraux détritiques d'échantillons individuels servent à préciser les âges stratigraphiques mal définis des formations comprises dans le supergroupe. Les âges de grains individuels de la Formation d'Imperial varient entre 650 et 350 Ma, avec un mode se situant entre 425 et 400 Ma, qui correspond au moment de la collision entre le protocontinent nord-américain et une masse continentale septentrionale au cours du Dévonien. Ces nouvelles données nous permettent de réévaluer nos connaissances actuelles sur les voies à la fois post-grenvilliennes et pré-ellesmériennes de transport des minéraux, depuis leurs sources jusqu'aux lieux de dépôt, pour les strates silicoclastiques du corridor du Mackenzie.

INTRODUCTION

The central Mackenzie River corridor is flanked by the 950 km long Mackenzie Mountains (Fig. 1), a fold-thrust belt with convex-eastward geometry that formed as a consequence of Late Cretaceous through Tertiary compression (MacNaughton et al., 2008). Structurally, the fold-thrust belt is characterized by broad anticlines cored by Neoproterozoic strata and narrow synclines of Paleozoic strata formed above a deep-seated detachment in the underlying basement (Cook and MacLean, 1999). The stratigraphic record of the region (e.g. Williams, 1990) illustrates a history of repeated vertical tectonism as evidenced by a series of trough and arch systems that were periodically active throughout the Phanerozoic. Movement of these structures over time has caused differential deposition and erosion throughout the region and consequently has a strong control on regional reservoir potential (Issler et al., 2005). Understanding the provenance, age, and depositional history of the strata helps to lend insight into regional geodynamics.

So far, understanding of the changing paleogeographic and tectonic setting of the Northern Cordillera in Canada is fairly limited. The prevailing model includes the formation of a major Paleozoic carbonate platform along the western passive margin of Laurentia following Neoproterozoic rifting of the earlier supercontinent (Lemieux et al., 2011). This was interrupted between 420–330 Ma as North America and Greenland collided with a ribbon continent and developed a thick Devonian siliciclastic succession throughout much of the Arctic (Patchett et al., 1999). Whereas regional detrital zircon U-Pb studies provide valuable information as to crystallization dates in a source area of sediments, the refractory nature of the mineral does not allow it to record the potentially several cycles of subsequent deposition. Muscovite, however, is much more susceptible to abrasion during transport and, thus, is most commonly a monocyclic detrital phase. As a result, $^{40}\text{Ar}/^{39}\text{Ar}$ dating of muscovite can yield valuable information on provenance in sedimentary systems (Reynolds et al., 2012).

Presented herein are muscovite $^{40}\text{Ar}/^{39}\text{Ar}$ data from eight Neoproterozoic and Devonian samples in the Mackenzie Mountains. Analysis of these ages provides key information

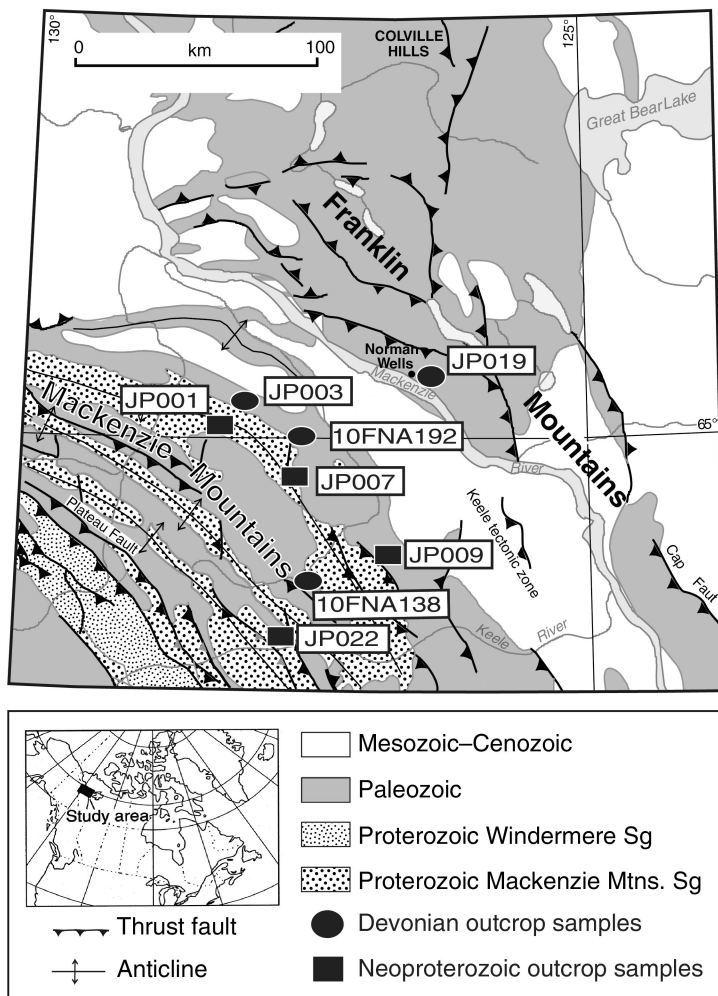


Figure 1. Location of study area and samples for detrital muscovite $^{40}\text{Ar}/^{39}\text{Ar}$ geochronology (modified from MacLean and Cook, 1999). Published with permission of the Canadian Society of Petroleum Geologists.

on the protracted depositional and tectonic history of the Mackenzie region throughout the Neoproterozoic and Paleozoic.

GEOLOGICAL SETTING

Neoproterozoic continental margin

The Proterozoic stratigraphic assemblage of Western and Northern Canada is thought to be comprised of three separate stratigraphic packages (A, B, C) separated by major subaerial unconformities (ca. 1200 Ma, 750 Ma respectively). Of these three packages, B and C are preserved in the Mackenzie Mountains as the Mackenzie Mountains Supergroup and Windermere Supergroup (Young et al., 1979). The strata recorded in these two supergroups have significantly different tectonic and depositional histories, and represent a change from a shallow intracontinental basin to passive margin deposition.

The Mackenzie Mountains Supergroup is mostly composed of shallow-water siliciclastic and carbonate units (Narbonne and Aitken, 1995). Whereas the configuration and dynamics of the basin are poorly understood, it is thought that sediments were deposited in a shallow epicratonic sea formed as a response to either failed rift-driven subsidence or crustal thinning related to passive margin formation. The stratigraphic thickness of the Mackenzie Mountains Supergroup varies from 4 km to 6 km, with formations thickening toward the southwest. Abrupt lateral changes in sedimentary facies and stratigraphic thickness are common throughout the region and this relationship has been interpreted as a response to the increased accommodation space over extensional half-grabens (Turner and Long, 2008). Isopach maps suggest that deposition occurred along a continental margin with a similar arcuate shape to the modern configuration of the mountain front. It is likely that the Proterozoic basin orientation played a strong control on modern structural configuration (Aitken and Long, 1978).

Classically, the Mackenzie Mountains Supergroup has been divided into four separate units (Fig. 2): map unit H1, Tsezotene Formation, Katherine Formation, and Little Dal Formation. The sandstone, shale, and dolostone units of map unit H1 are the oldest strata exposed in the region and lie unconformably on top of deformed Mesoproterozoic strata (Narbonne and Aitken, 1995). The Tsezotene and Katherine formations represent a large coarsening-upward cycle from a mudstone-dominated shelf to the mostly terrigenous Katherine Formation (Turner and Long, 2008). Finally, the Little Dal Formation comprises carbonate and evaporite rocks with a basal siliciclastic “Mudcracked Unit” (Narbonne and Aitken, 1995). A suite of diabase dykes and sills were intruded through the Tsezotene and Little Dal formations and follow a parallel orientation to the extensional faults that influence the stratigraphic thickness of the overlying Windermere Supergroup (Armstrong et al., 1982). These

intrusions are geochemically similar to basaltic lava flows found at the top of the Little Dal Formation and likely correspond to the initiation of Neoproterozoic rifting and the breakup of Laurentia (Jefferson and Parrish, 1989).

A U-Pb detrital zircon age (1079 ± 2 Ma; Narbonne and Aitken, 1995) from the upper Katherine Formation serves to constrain the maximum deposition age of the unit and is within error of the youngest detrital ages from the Nelson Head Formation (1077 ± 2 Ma), an analogous unit on Victoria Island (Macdonald et al., 2012). Additional corroboration (1267 ± 2 Ma; 1175–1100 Ma) is provided by U-Pb dating of baddeleyite from the Copper Creek lavas that are unconformably overlain by Mackenzie Mountains Supergroup correlatives and basement-derived granitic clasts in diatremes that crosscut the Mackenzie Mountains Supergroup (Narbonne and Aitken, 1995). Minimum ages for the Mackenzie Mountains Supergroup were determined through Rb-Sr dating of the Tsezotene sills (766 ± 24 Ma; 769 ± 27 Ma; Armstrong et al. (1982)) and U-Pb dating of the granitic diatreme that intrudes the Little Dal Formation ($778 \pm 3/-2$ Ma). The geochemical similarities between these igneous bodies and the basaltic lava flow that caps the Little Dal Formation indicate that the ages likely provide the stratigraphic age for the top of the Mackenzie Mountains Supergroup (Jefferson and Parrish, 1989).

In the Mackenzie Mountains, Proterozoic sequence C is recorded in the rift deposits of the Windermere Supergroup. Conglomerate, evaporate, and glacial diamictite units characterize the basal units of this succession the expression of which is confined to inferred syndepositional rift valleys. Younger Windermere Supergroup siliciclastic and carbonate units were deposited on the shelf of a passive margin and are significantly more extensive than the rift deposits over which they lie (Narbonne and Aitken, 1995). Regionally, the Windermere Supergroup is mostly confined to the area west of the Mackenzie Arch, a northwest-trending regional erosional surface active from the Late Proterozoic through the Late Cambrian (Williams, 1990).

Paleozoic transgression

In the vicinity of the Mackenzie Mountains, Cambrian strata unconformably overlie strata of the Mackenzie Mountains Supergroup, and seismic interpretation suggests that deposition was syntectonic into grabens (Hadlari et al., 2012). Throughout the Cambrian the Mackenzie Arch was still a regional surface of erosion and nondeposition and as a result, Cambrian strata thins to the southwest and is not present over the inferred location of the paleoarch (Williams, 1990). The Cambrian stratigraphy east of the Mackenzie Arch records the ongoing Cambrian transgression with the depositional environment evolving from a subtidal and evaporitic basin to an open marine shelf (Pyle and Gal, 2009a). From the latest Cambrian through Devonian, a major carbonate platform developed on top of this shelf during continued transgression of the Cambrian evaporitic basin. Facies

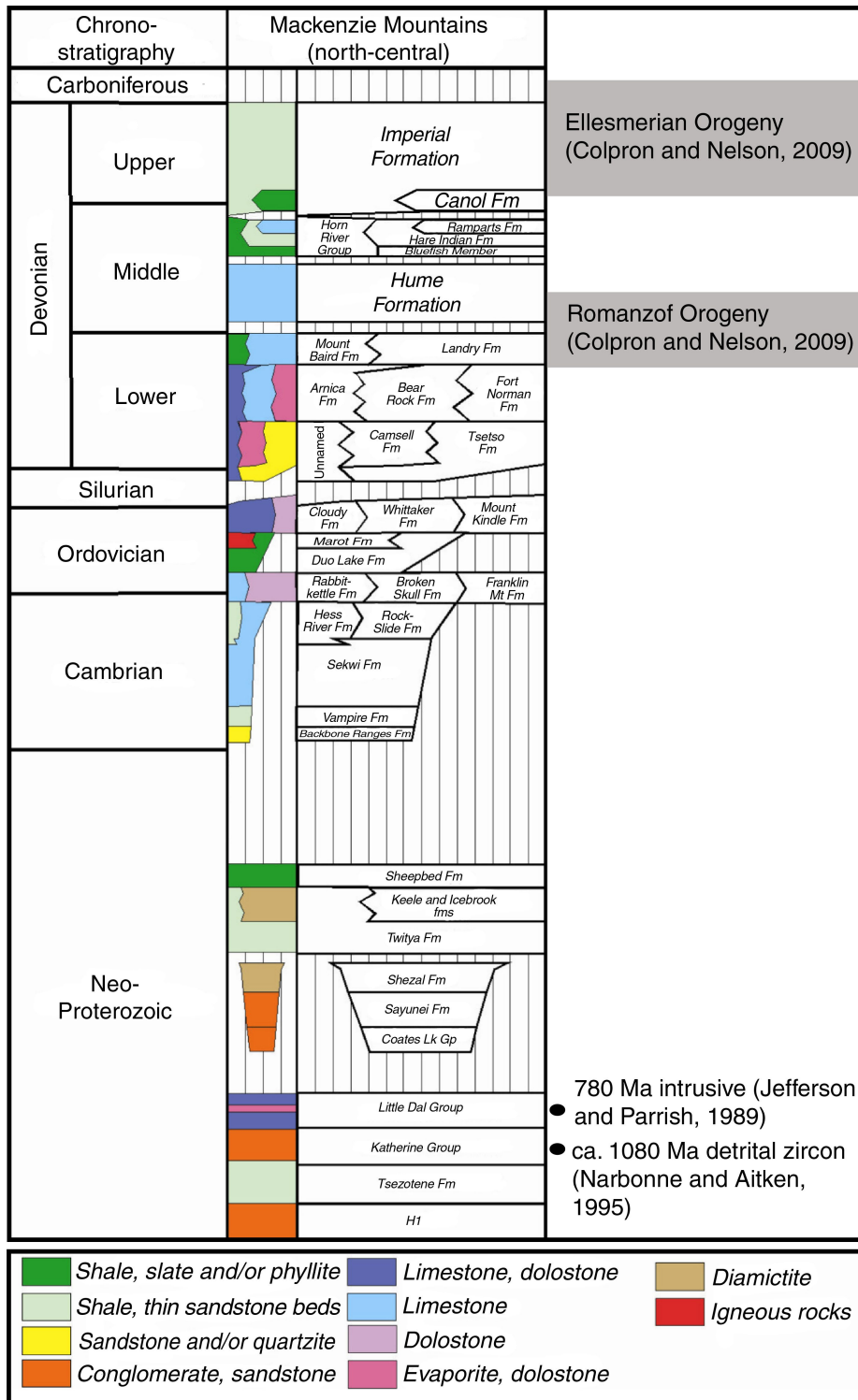


Figure 2. Stratigraphic column for the north-central Mackenzie Mountains (modified from MacNaughton et al., 2008).

variations, paleotopographic highs and erosional surfaces, and a lack of drill core that penetrates the Lower Paleozoic section makes it difficult to estimate the average thickness of Paleozoic strata throughout the region; however, on the basis of maximum observed unit thicknesses, a conservative estimate would be less than 4 km of Paleozoic carbonate strata overlying the Mackenzie Mountains Supergroup throughout the Mackenzie River corridor (Pyle and Gal, 2009a, b; Gal and Pyle, 2009; Gal et al., 2009).

The rapid change from the platform carbonate of the Middle Devonian Hume Formation to shale of the Horn River Group marks another major transgressive pulse and drowning of the carbonate platform (Gal et al., 2009). This transgression continued into the Late Devonian (Frasnian), when collision of a northern landmass with Laurentia resulted in pronounced uplift in the source regions and the progradation of the clastic Imperial Formation (Gentzis and Goodarzi, 1993). These siltstone and sandstone components form a fan-slope complex attached to a basin margin in the east and thicken to the southwest (Hadlari et al., 2009). Detrital zircon U-Pb ages from the Imperial Formation show that provenance is mostly sourced from northern Laurentia, with potential input from a northern exotic terrane due to a 700–500 Ma age population that is not present in the Laurentian magmatic record. The detrital signature records a shift in the Upper Devonian–Lower Carboniferous, suggesting a change in provenance (Lemieux et al., 2011).

Late Paleozoic–Mesozoic depositional history

A major regional unconformity exists between the Upper Devonian Imperial Formation and Albian strata. Missing stratigraphic section elsewhere in Northern Canada indicates that there were likely several cycles of deposition and erosion throughout this period (Williams, 1990). Integration of stratigraphic, apatite fission track, and thermal maturity data from a well in the Brackett Basin suggests that a section between 2.5 km and 3.5 km in thickness was removed prior to the formation of a Cretaceous foreland basin in the Albian (Issler et al., 2005).

METHODS AND RESULTS

Samples for this study were collected along an approximately 160 km traverse from the Mackenzie Mountains through the Mackenzie Plain to the southwest flank of the Franklin Mountains (Fig. 1). Our sampling strategy was intended to survey a broad stratigraphic and geographic range to assess spatial and temporal patterns in the detrital record ages. In particular, targeted units included the Neoproterozoic siliciclastic formations that form the cores of anticlines in the fold thrust belt and the Paleozoic and Mesozoic siltstone and sandstone units found along the mountain front and throughout the Mackenzie Plain. At each sample locality, 2–5 kg of sample was collected for

$^{40}\text{Ar}/^{39}\text{Ar}$ muscovite geochronology. From these forty-six samples, four Neoproterozoic and four Devonian samples were selected for preliminary investigation.

Muscovite samples for $^{40}\text{Ar}/^{39}\text{Ar}$ dating were obtained via standard crushing and separation techniques. Hand samples were crushed in the jaw crusher at the University of Ottawa (Ottawa, Ontario), sieved to a 105–500 μm size fraction, cleaned in water and acetone, and set to dry overnight. From this, several dozen alteration-free muscovite grains were hand-picked under a binocular microscope. Individual grains were loaded into holes machined into aluminum disks and irradiated for 85 hours at the USGS TRIGA reactor (Denver, Colorado, U.S.A.). For this study, Fish Canyon Tuff sanidine (FCT) was adopted as the neutron flux monitor (apparent age: 28.02 Ma; Renne et al. (1998)). Samples and FCT flux monitor were isotopically analyzed at New Mexico Tech (Socorro, New Mexico, U.S.A.). Argon from individual grains was extracted with a 75 W Photon-Machines CO_2 laser in an automated, all-metal extraction line. Isotopic analyses were conducted on an ARGUS VI mass spectrometer; *see* Table 1 for complete analytical details. Data for individual samples are presented here as histograms plotted with a bin size of 25 Ma and their associated cumulative probability plots (Fig. 3, 4) calculated using ISOPLOT 4.0 (Ludwig, 2008). The present authors analyzed approximately 25 individual crystals per sample, performing total-fusion analyses for each grain. A limitation of this approach is that it was not possible to assess the argon systematics within the muscovite, and as a result, the age data do not provide any method to assess argon loss or uptake. Given the detrital nature of the samples, this limitation should not hinder the geological interpretation.

Detrital muscovite $^{40}\text{Ar}/^{39}\text{Ar}$ ages, sample locations, and analytical data for all eight samples are presented in Table 1.

Ages for both the Neoproterozoic and Devonian strata have been plotted on a cumulative histogram (Fig. 3). For the samples from the Mackenzie Mountains Supergroup, the single crystal ages exhibit a unimodal population, with a ca. 1075 Ma mode. A majority of the single-grain ages from the Devonian strata occur between 500 Ma and 400 Ma, and a ca. 425 Ma mode.

Neoproterozoic samples

Age distributions for the four Neoproterozoic samples are presented in increasing stratigraphic order in Figure 4. Both samples JP001 and JP022 were collected from the Tsezotene Formation; however, JP001 was sampled from directly below the contact with the overlying Katherine Formation and is inferred to be the stratigraphically younger of the two samples. Generally, these sandstone samples are fine- to medium-grained quartz arenite with no observable porosity due to extensive quartz overgrowth and iron-oxide cements. Petrographically, it is apparent that the strata have undergone significant compaction as evidenced by the sutured contacts,

Table 1. Single-crystal total fusion $^{40}\text{Ar}/^{39}\text{Ar}$ analyses of muscovite from the Mackenzie Mountains, Northwest Territories.

ID	$^{40}\text{Ar}/^{39}\text{Ar}$	$^{37}\text{Ar}/^{39}\text{Ar}$	$^{36}\text{Ar}/^{39}\text{Ar}$ ($\times 10^{-3}$)	$^{39}\text{Ar}_K$ ($\times 10^{-15}$ mol)	$^{40}\text{Ar}^*$ (%)	Age (Ma)	$\pm 1\sigma$ (Ma)
JP001: Tsezotene Fm (quartz wacke) UTM (NAD83): 65.019710, -127.809619; J: 0.018399							
11	40.81	-0.031	0.947	0.892	99.3	1005.0	1.8
03	42.86	-0.038	1.208	0.648	99.2	1042.1	2.3
08	43.17	-0.147	1.052	1.035	99.3	1048.5	1.4
15	43.23	0.020	0.775	0.960	99.5	1051.5	1.7
25	43.58	-0.012	1.287	0.612	99.1	1055.1	2.6
23	43.81	0.002	1.143	0.886	99.2	1060.1	1.8
17	44.12	-0.133	0.934	0.885	99.3	1066.7	2.0
02	44.15	-0.001	0.835	1.267	99.4	1068.1	1.2
18	44.69	-0.082	2.422	0.367	98.4	1069.2	4.2
16	44.82	-0.059	2.838	0.312	98.1	1069.4	5.2
21	44.47	0.047	1.597	0.503	98.9	1069.9	3.2
05	44.25	-0.012	0.789	1.793	99.5	1070.1	1.0
13	44.34	-0.022	0.802	1.019	99.5	1071.6	1.8
04	44.50	0.041	1.248	0.686	99.2	1072.2	2.6
24	44.66	-0.025	1.457	0.535	99.0	1073.9	3.1
10	44.62	-0.012	1.110	0.773	99.3	1075.1	1.9
22	44.65	0.020	1.234	0.804	99.2	1075.1	2.0
14	44.62	0.009	0.929	2.296	99.4	1076.2	0.8
06	44.78	-0.009	0.637	3.179	99.6	1080.6	0.6
12	45.30	-0.011	2.024	0.676	98.7	1082.7	2.3
20	45.15	-0.018	0.980	0.793	99.4	1085.6	2.3
01	51.70	-0.041	2.002	1.226	98.8	1195.7	1.6
07	61.31	-0.001	1.121	0.867	99.5	1357.1	2.2
19	163.2	-0.098	1.431	0.622	99.7	2498.9	4.7
09	169.8	0.018	0.685	1.192	99.9	2554.2	2.3
JP007: Little Dal Fm (quartz arenite) UTM (NAD83): 64.895236, -127.250024; J: 0.018409							
20	31.44	0.026	0.960	1.637	99.1	817.8	0.9
01	33.97	0.001	1.347	2.132	98.8	867.9	0.8
25	33.97	-0.006	1.040	1.344	99.1	869.7	1.0
08	34.35	0.046	1.479	2.784	98.7	875.1	1.0
06	34.74	0.029	1.085	5.546	99.1	885.3	0.7
21	35.51	-0.007	1.067	1.736	99.1	901.1	0.9
19	35.51	0.043	0.935	1.188	99.2	901.8	1.2
09	35.58	0.026	0.444	9.492	99.6	906.2	0.6
17	35.70	0.003	0.545	3.844	99.5	907.9	0.4
07	36.88	0.047	2.628	2.465	97.9	919.4	1.0
23	36.78	-0.003	0.609	2.384	99.5	929.1	0.6
11	37.30	0.004	1.675	2.683	98.7	933.1	0.5
22	37.50	0.019	1.493	1.479	98.8	938.2	0.9
05	37.73	0.015	0.977	3.776	99.2	945.7	0.5
16	38.84	0.024	1.278	1.509	99.0	965.8	1.0
13	39.28	0.003	0.633	5.497	99.5	977.8	0.4
24	39.83	0.019	1.252	1.428	99.1	985.0	1.1
10	41.93	0.000	2.183	0.987	98.5	1019.7	1.6
04	42.27	0.019	0.938	1.694	99.3	1033.1	1.0
03	43.04	0.029	1.191	1.340	99.2	1046.0	1.2
12	42.97	0.008	0.765	2.343	99.5	1047.1	0.7
14	44.05	0.004	0.449	4.585	99.7	1068.7	0.4
15	44.64	0.009	1.127	2.644	99.3	1075.9	0.6
02	47.34	0.010	0.822	1.838	99.5	1126.2	1.0

Table 1. (cont.)

ID	⁴⁰ Ar/ ³⁹ Ar	³⁷ Ar/ ³⁹ Ar	³⁶ Ar/ ³⁹ Ar (x10 ⁻³)	³⁹ Ar _K (x10 ⁻¹⁵ mol)	⁴⁰ Ar* (%)	Age (Ma)	±1σ (Ma)
JP009: lower Katherine Fm (quartz arenite) UTM (NAD83): 64.474943, -126.882328; J: 0.018409							
15	38.68	0.044	1.173	1.102	99.1	963.3	1.3
09	38.94	0.047	1.859	0.715	98.6	964.3	2.3
14	38.71	-0.002	0.876	2.357	99.3	965.4	0.7
12	38.86	-0.002	1.165	2.534	99.1	966.7	0.6
21	39.08	0.086	0.824	1.603	99.4	973.2	1.1
24	40.22	0.058	3.391	0.895	97.5	980.5	1.8
02	39.53	-0.103	0.898	1.359	99.3	981.0	1.1
10	40.25	0.035	1.945	0.609	98.6	989.3	2.7
01	39.95	-0.034	0.767	2.653	99.4	989.9	0.7
03	39.96	-0.022	0.657	3.826	99.5	990.9	0.5
11	40.16	0.014	1.195	0.989	99.1	991.6	1.5
05	41.31	0.002	0.699	3.009	99.5	1016.3	0.5
17	42.81	0.017	0.947	1.433	99.3	1043.2	1.3
13	43.18	-0.017	1.215	1.572	99.2	1048.4	1.1
19	43.75	0.017	1.423	1.066	99.0	1058.0	1.7
22	43.97	0.010	1.336	1.334	99.1	1062.4	1.2
06	44.11	-0.011	0.839	2.144	99.4	1067.6	0.8
04	44.46	-0.004	1.190	1.710	99.2	1072.2	1.0
20	46.81	0.037	1.074	1.050	99.3	1115.5	1.6
07	47.05	-0.003	0.618	2.409	99.6	1122.1	0.7
26	47.87	-0.024	1.208	0.957	99.3	1133.5	1.8
23	48.04	-0.031	1.169	1.074	99.3	1136.8	1.6
16	48.02	-0.011	0.967	1.205	99.4	1137.5	1.5
18	48.35	0.012	1.887	1.508	98.8	1138.6	1.2
25	48.35	0.029	0.772	1.304	99.5	1144.4	1.4
08	49.21	-0.014	0.752	1.538	99.5	1159.5	1.3
JP022: Tsezotene Fm (quartz arenite) UTM (NAD83): 64.157116, -128.099835; J: 0.018402							
17	18.22	0.012	2.743	0.286	95.6	501.2	3.1
24	40.02	0.011	0.644	1.504	99.5	991.9	1.0
11	41.34	0.009	0.847	0.976	99.4	1015.8	1.6
26	42.14	0.005	0.519	2.012	99.6	1032.7	0.8
23	42.60	0.016	1.285	0.853	99.1	1037.0	1.8
22	43.13	-0.018	1.186	1.071	99.2	1047.4	1.4
18	43.16	0.015	1.097	0.743	99.3	1048.4	2.3
13	43.10	0.018	0.635	1.473	99.6	1049.9	1.2
Notes: Isotopic ratios corrected for blank, radioactive decay, and detector calibrations not corrected for interfering reactions. Errors quoted for individual analyses include analytical error only, without interfering reaction or J uncertainties. Error on J = ± 0.004% Decay constants and isotopic abundances after Steiger and Jäger (1977). Ages calculated relative to FC-2 Fish Canyon Tuff sanidine interlaboratory standard at 28.02 Ma. Decay constant (λK (total)) = 5.543e-10/a IC = Measured (⁴⁰ Ar/ ³⁶ Ar)/295.5 No ³⁷ Ar detected above background. Correction factors: (³⁹ Ar/ ³⁷ Ar)Ca = 0.0006953 ± 1e-06 (³⁶ Ar/ ³⁷ Ar)Ca = 0.0002785 ± 2e-7 (⁴⁰ Ar/ ³⁹ Ar)K = 0.007951 ± 6.4e-05							

Table 1. (cont.)

ID	$^{40}\text{Ar}/^{39}\text{Ar}$	$^{37}\text{Ar}/^{39}\text{Ar}$	$^{36}\text{Ar}/^{39}\text{Ar}$ ($\times 10^{-3}$)	$^{39}\text{Ar}_K$ ($\times 10^{-15}$ mol)	$^{40}\text{Ar}^*$ (%)	Age (Ma)	$\pm 1\sigma$ (Ma)
25	43.12	0.033	0.606	1.362	99.6	1050.5	1.1
08	43.42	0.047	0.726	1.142	99.5	1055.4	1.5
07	43.54	-0.027	0.629	2.315	99.6	1058.1	0.8
12	43.67	0.001	0.733	1.667	99.5	1060.0	1.0
16	44.01	-0.005	0.451	2.240	99.7	1067.7	0.7
04	44.87	-0.033	0.574	1.902	99.6	1082.7	0.9
03	44.85	0.008	0.319	5.146	99.8	1083.8	0.3
05	45.35	0.000	0.596	2.123	99.6	1091.4	0.8
06	45.80	0.072	0.654	1.845	99.6	1099.3	0.9
20	45.96	-0.001	0.631	1.410	99.6	1102.2	1.1
21	46.41	0.034	0.821	0.910	99.5	1109.4	1.9
02	46.62	0.016	0.364	6.241	99.8	1115.5	0.3
10	46.80	0.001	0.543	1.863	99.7	1117.8	0.9
09	47.14	-0.088	0.902	1.107	99.4	1121.7	1.6
19	47.71	0.030	0.991	1.086	99.4	1131.6	1.7
15	47.83	0.015	1.091	1.130	99.3	1133.2	1.6
01	48.52	0.010	0.360	7.089	99.8	1149.1	0.3
14	49.77	-0.004	0.304	3.508	99.8	1171.3	0.6
JP003: Imperial Fm (quartz wacke) UTM (NAD83): 65.112148, -127.855016; J: 0.018402							
12	13.86	-0.247	3.556	0.190	92.3	381.0	3.6
21	15.61	0.127	7.410	0.273	86.0	398.2	2.7
06	13.86	0.058	1.337	0.570	97.2	399.3	1.2
23	14.09	0.129	1.474	0.462	97.0	404.6	1.5
09	14.32	-0.009	2.193	0.341	95.5	404.7	2.3
08	14.31	0.061	1.483	0.459	97.0	410.1	1.6
07	14.22	0.069	0.886	0.806	98.2	412.4	0.9
24	14.40	0.125	1.411	0.478	97.2	413.2	1.6
04	15.09	0.150	2.118	0.444	95.9	426.0	1.7
02	15.10	0.091	1.571	0.450	97.0	430.2	1.7
25	15.29	0.095	1.620	0.470	96.9	434.9	1.8
17	15.20	0.325	1.278	0.566	97.7	435.7	1.5
18	15.57	0.156	2.013	0.408	96.3	439.3	2.0
03	15.53	0.062	1.165	0.661	97.8	444.6	1.4
01	16.70	0.031	0.570	1.945	99.0	479.1	0.5
15	18.07	-0.003	2.482	0.279	95.9	499.3	3.0
14	17.92	0.108	1.764	0.419	97.1	501.1	2.2
20	18.14	-0.029	2.166	0.332	96.5	503.3	2.8
05	18.17	0.112	1.414	0.514	97.7	509.9	1.8
11	18.72	0.065	2.041	0.346	96.8	519.1	2.6
19	18.68	0.130	0.970	0.723	98.5	526.0	1.3
22	18.85	0.094	0.867	0.879	98.7	530.9	1.1
10	20.86	0.078	1.254	0.574	98.3	577.3	1.8
13	83.93	0.017	1.512	0.451	99.5	1679.0	5.0
JP019: Imperial Fm (siltstone) UTM (NAD83): 65.266101, -126.738284; J: 0.01839							
07	1.774	0.003	1.402	0.621	76.6	44.3	0.4
09	13.81	0.311	4.583	0.151	90.4	372.5	4.2
08	14.93	0.084	3.352	0.203	93.4	411.7	3.7
04	14.46	-0.050	1.312	0.570	97.3	414.8	1.4

Table 1. (cont.)

ID	⁴⁰ Ar/ ³⁹ Ar	³⁷ Ar/ ³⁹ Ar	³⁶ Ar/ ³⁹ Ar (x10 ⁻³)	³⁹ Ar _K (x10 ⁻¹⁵ mol)	⁴⁰ Ar* (%)	Age (Ma)	±1σ (Ma)
02	15.21	0.066	1.038	0.794	98.0	437.0	0.9
05	15.76	-0.027	2.638	0.269	95.0	438.6	3.0
03	18.05	-0.178	2.241	0.288	96.2	499.9	3.3
06	19.17	0.172	3.072	0.226	95.3	522.5	4.2
01	35.94	0.047	0.960	1.337	99.2	909.6	1.1
10FNA192A02: Imperial Fm (lithic arenite) UTM (NAD83): 64.385464, 127.534522; J: 0.018411							
07	14.26	-0.271	5.128	0.155	89.2	379.5	4.6
09	13.77	-0.101	2.706	0.287	94.1	385.8	2.5
13	14.52	0.039	4.825	0.158	90.2	389.6	4.7
01	14.20	0.044	1.106	0.936	97.7	410.2	1.0
06	14.78	0.047	2.290	0.386	95.4	416.3	1.9
11	14.81	0.005	2.175	0.349	95.7	417.9	2.3
05	17.46	0.017	4.075	0.187	93.1	472.3	4.6
04	17.07	-0.022	2.233	0.450	96.1	476.1	1.9
12	17.53	0.046	3.458	0.253	94.2	478.7	3.3
08	17.62	-0.145	3.298	0.235	94.4	481.7	3.5
02	17.34	-0.107	1.425	0.609	97.5	488.8	1.4
03	19.56	0.026	1.648	0.530	97.5	542.9	1.7
14	83.54	-0.261	3.350	0.222	98.8	1666.8	9.2
10	176.0	0.004	0.601	1.554	99.9	2604.6	2.0
10FNA138B01: Imperial Fm (siltstone) UTM (NAD83): 64.51699, 127.948148; J: 0.01838							
14	14.62	0.356	6.919	0.116	86.2	375.7	5.9
02	14.19	0.051	1.235	0.550	97.5	408.4	1.3
06	14.60	-0.018	0.839	2.060	98.3	422.1	0.4
11	15.73	0.129	2.643	0.314	95.1	438.0	2.8
03	15.28	-0.003	0.636	1.235	98.8	441.5	0.8
01	19.86	0.028	0.903	1.327	98.7	554.7	0.8
12	23.02	0.170	2.354	0.300	97.0	620.4	3.8
05	23.31	0.086	1.145	0.740	98.6	635.3	1.6
10	23.83	0.092	2.715	0.340	96.7	636.8	3.4
09	29.40	-0.152	2.825	0.230	97.1	760.9	5.7
13	151.6	0.057	1.922	0.381	99.6	2397.1	7.3
07	172.6	0.011	0.960	0.862	99.8	2575.0	3.0
04	173.3	-0.013	0.845	1.850	99.9	2580.5	1.4
Notes: Isotopic ratios corrected for blank, radioactive decay, and detector calibrations not corrected for interfering reactions. Errors quoted for individual analyses include analytical error only, without interfering reaction or J uncertainties. Error on J = ± 0.004% Decay constants and isotopic abundances after Steiger and Jäger (1977). Ages calculated relative to FC-2 Fish Canyon Tuff sanidine interlaboratory standard at 28.02 Ma. Decay constant (λK (total)) = 5.543e-10/a IC = Measured (⁴⁰ Ar/ ³⁶ Ar)/295.5 No ³⁷ Ar detected above background. Correction factors: (³⁹ Ar/ ³⁷ Ar)Ca = 0.0006953 ± 1e-06 (³⁶ Ar/ ³⁷ Ar)Ca = 0.0002785 ± 2e-7 (⁴⁰ Ar/ ³⁹ Ar)K = 0.007951 ± 6.4e-05							

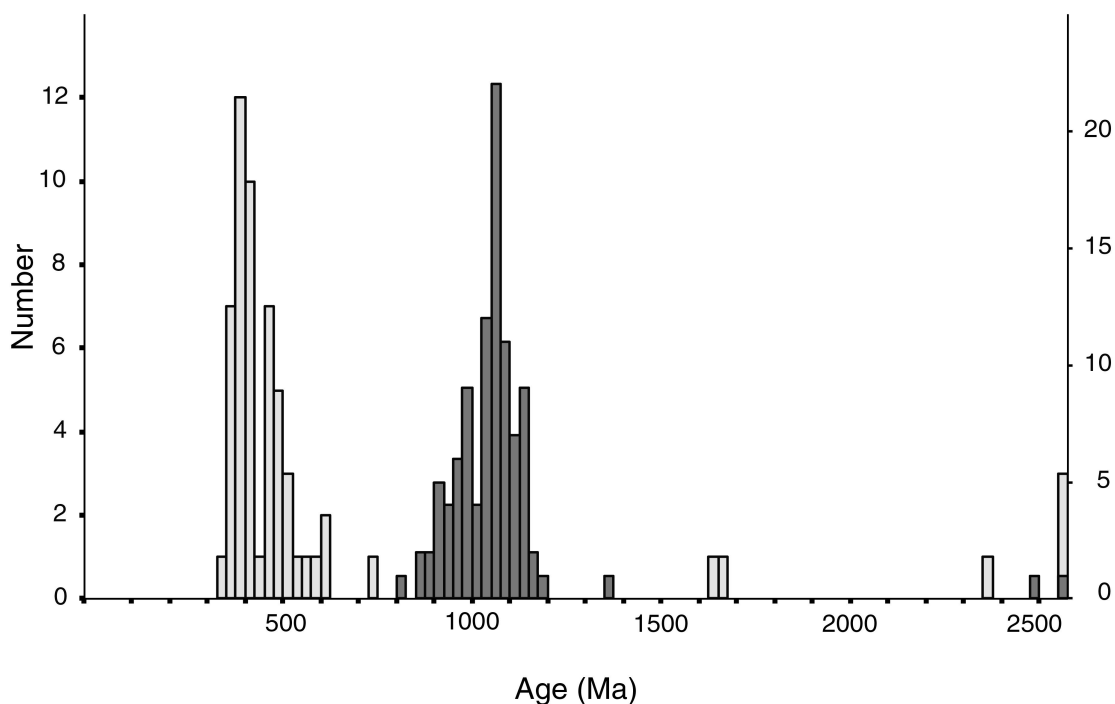


Figure 3. Cumulative histogram of detrital muscovite $^{40}\text{Ar}/^{39}\text{Ar}$ ages for samples from the Devonian Imperial Formation (light grey, left y axis) and Neoproterozoic Mackenzie Mountains Supergroup (dark grey, right y axis).

pervasive stylolites, and deformed mica grains (Fig. 5a, 5b). Sample JP001 differs from the other three samples as it is a poorly sorted quartz wacke. Sample JP007 is from the basal Little Dal Formation and is finer grained and more hematitic than the other samples. Mineralogically, it differs from the older siliciclastic rocks due the relative abundance of garnet, clinozoisite, and other detrital metamorphic minerals.

Ages for muscovite from JP001 and JP022 are normally distributed with a mean age of ca. 1100 Ma. The youngest grain age for samples from the Tsezotene Formation is recorded in sample JP022 (992 ± 1 Ma). A small number of grains in sample JP001 are significantly older than the other measurements and may represent another detrital population (ca. 2500 Ma). The ages in sample JP009 from the Lower Katherine Formation do not exhibit the same normal distribution as samples JP001 and JP022. Instead, three major populations are observed (ca. 1000–950 Ma, 1075 Ma, 1150–1100 Ma). Sample JP007 yielded the youngest muscovite grains, with a majority dated between 950 Ma and 850 Ma, and a youngest age of 817 ± 1 Ma.

Devonian samples

Figure 4 shows the distribution of ages in the four samples from the Imperial Formation. Unfortunately, detailed information on their relative stratigraphic position is unknown thus the results are not arranged in any chronological order. Samples JP003 and JP019 were collected by the authors,

whereas samples 10FNA192A02 and 10FNA138B01 were provided by K. Fallas (Geological Survey of Canada). Sample JP003 is a finely laminated, fine-grained quartz wacke. Quartz grains are subangular to subrounded, loosely packed and mostly cemented by calcite cement. A minor secondary porosity exists due to dissolution of the cement and alteration of the matrix clay minerals. Sample JP019 is a siltstone with abundant organic matter. Calcite cement is present, but is secondary to iron-oxide cement (Fig. 5c, 5d). Muscovite is less common and smaller than in sample JP003 and lacks any preferred orientation. Sample 10FNA138B01 is a crosslaminated, silt to fine-grained lithic arenite with horizontal burrows; sample 10FNA192A02 is a micaceous, fine-grained, parallel-laminated lithic arenite also with horizontal burrows. Muscovite from all four samples is relatively fine and heavily disaggregated into small, single sheets.

Fewer grains were analyzed in each of the four Devonian samples due to poor recovery of appropriately sized muscovite. The majority of detrital ages in all four samples occur between 500 Ma and 400 Ma, and possess a 425–400 Ma mode. Sample 10FNA138B01 has a bimodal distribution of ages, with an older population between 675 Ma and 575 Ma. Both samples 10FNA192A02 and 10FNA138B01 possess a few muscovite grains that record ca. 2550 Ma ages; samples JP003 and 10FNA192A02 have single grains with a ca. 1650 Ma age. Of the four Devonian samples, the youngest $^{40}\text{Ar}/^{39}\text{Ar}$ muscovite age (373 ± 4 Ma) analyzed was from

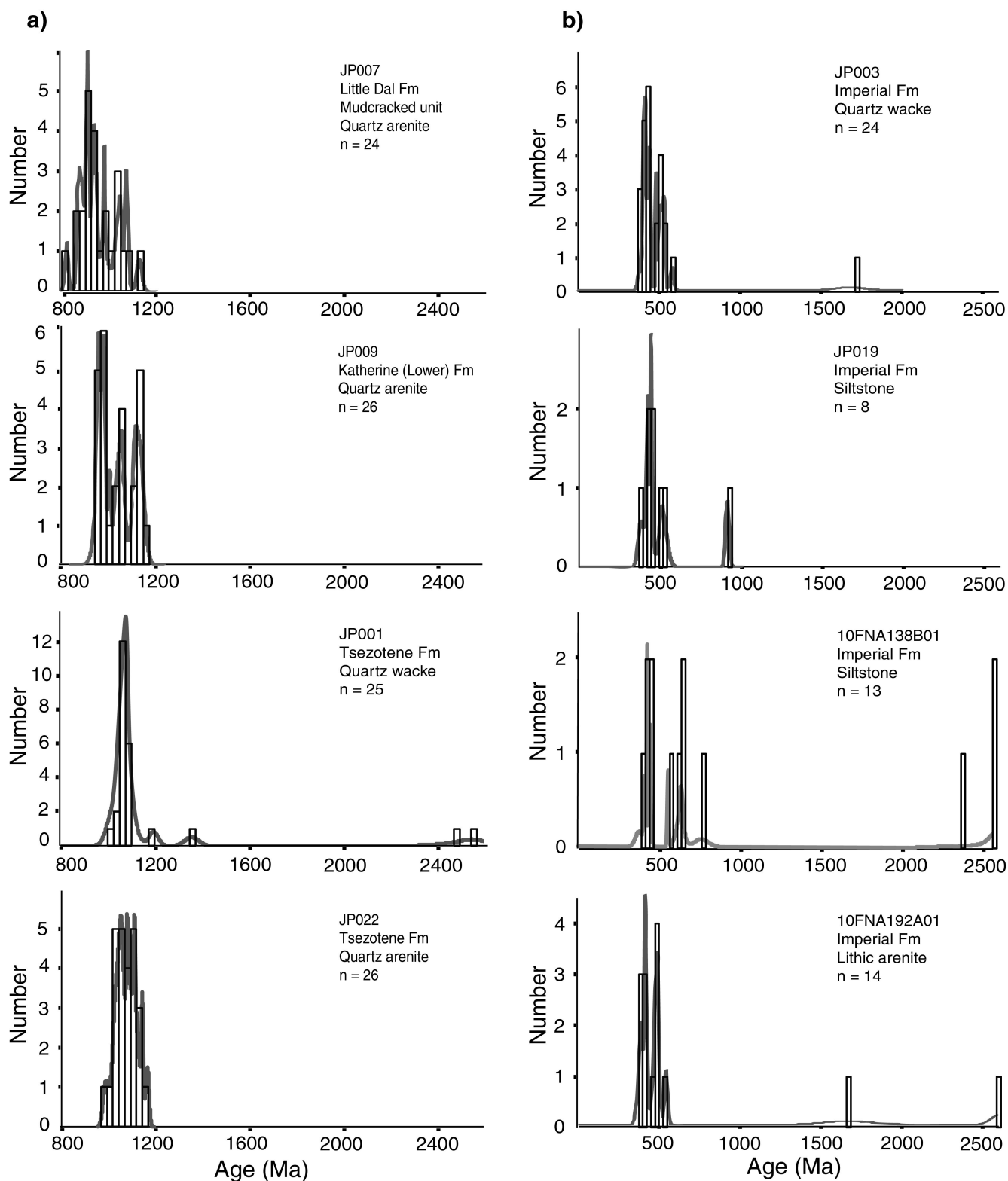


Figure 4. Histograms and density probability plots (25 Ma bin size) of detrital muscovite $^{40}\text{Ar}/^{39}\text{Ar}$ ages. **a)** Neoproterozoic units of the Mackenzie Mountains Supergroup. **b)** Samples from the Devonian Imperial Formation.

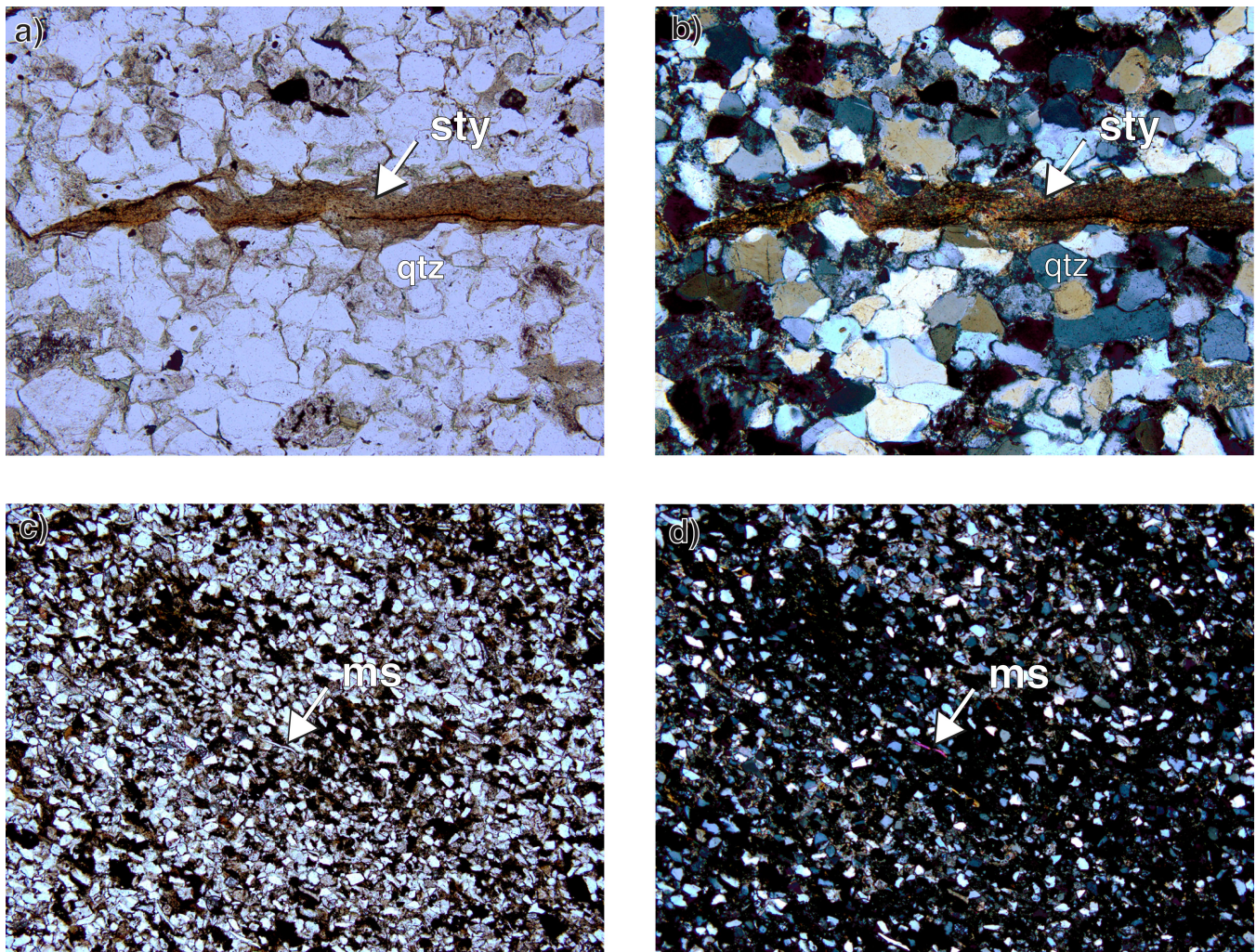


Figure 5. Photomicrographs of **a)** sample JP022, Tsezotene Formation showing deformation textures including stylolitic solution surface (sty) and sutured boundaries between interlocking quartz (qtz) grains; plain light; 2013-200; **b)** previous sample under crosspolarized light; 2013-202; **c)** sample JP019, Imperial Formation, with abundant clay and organic material serving as cement and matrix between silt-sized quartz grains; muscovite (ms) is abundant in the sample, but crystals are often small and abraded; plain light; 2013-203; **d)** previous sample under crosspolarized light. Field of view is 4 mm. 2013-201. All photographs by J. Powell.

siltstone sample JP019, with similarly young ages in sample 10FNA192A02 (380 ± 5 Ma) and sample 10FNA138B01 (375 ± 6 Ma).

Analyses from two grains yielded slightly anomalous ages: one from sample JP022 (501 ± 3 Ma) and the other from sample JP019 (44 ± 0.4 Ma). These $^{40}\text{Ar}/^{39}\text{Ar}$ muscovite ages are significantly younger than the other population of ages from their respective samples, as well as younger than their proposed depositional ages. These young ages are interpreted to be a result of alteration-driven alkali loss (Mitchell and Taka, 1984), consistent with petrographic observations of diagenetic alteration, and reflect neither a detrital age nor the timing of a postdepositional thermal event.

DISCUSSION

Laboratory experiments have determined that argon diffusion in muscovite is thermally controlled with a nominal closure temperature of between 350°C and 400°C (Harrison and Zeitler, 2005; Reiners and Brandon, 2006), which is moderately hotter than the upper boundary of the prehnite-pumpellyite metamorphic facies. If this temperature was achieved for a substantial duration by any of the samples while under burial conditions, a complex product of detrital and diagenetic (metamorphic) muscovite ages would be apparent (Adams and Kelley, 1998). Of the eight samples dated, none had populations younger than the proposed depositional age of the sample, allowing, with the exception of two anomalous ages, the present authors rule out $^{40}\text{Ar}/^{39}\text{Ar}$ muscovite ages related to diagenetic, metamorphic, or

other hydrothermal reheating of grains. Instead, the ages are indeed detrital and record the timing of cooling in the respective source terranes.

The detrital ages of the muscovite from the Imperial Formation come as no surprise, as organic thermal maturity parameters indicate that throughout the region, maximum paleotemperatures for the Imperial Formation fall within the oil and gas window. In addition, thickness estimates for the missing Paleozoic and Early Mesozoic section do not indicate sufficiently deep burial following the Devonian (Issler et al., 2005) to thermally reset argon systematics in muscovite; however, the detrital ages from the Neoproterozoic units were unexpected due to the fact that regional stratigraphic studies indicate that the Mackenzie Mountains Supergroup was a locus of rifting with consequent volcanism and elevated geothermal gradients. Moreover, the Mackenzie Mountains Supergroup has been buried to significant depths throughout the Neoproterozoic and Phanerozoic. Had the Mackenzie Mountains Supergroup achieved a moderate temperature to reset the muscovite chronometer, it is likely that the cooling ages would record Cretaceous Laramide tectonism.

Instead, detrital ages from the Mackenzie Mountains Supergroup strata detail cooling and unroofing in the source terrane prior to deposition in the Mackenzie Mountains Supergroup basin. As expected, the grain ages are progressively younger from the Tsezotene through the Little Dal Formations. In addition to the generally younger muscovite ages, the pattern of age distribution changes progressively upsection: the Tsezotene Formation samples have a single population of muscovite ages, whereas the Katherine and Little Dal formations have ages that are broadly distributed. This may reflect a tectonic change in the source region over time, with sediments sourced from a single, rapidly exhumed orogenic source during Tsezotene Formation deposition and a more slowly exhumed source in the time of Katherine Formation and Little Dal Formation deposition. Alternatively, the broad spread in ages in the Katherine Formation and Little Dal Formation samples may represent a switch from a single source in the Tsezotene Formation to multiple sources (Haines et al., 2004). An increase in the metamorphic mineral abundance in sample JP007 compared to the other samples supports the hypothesis of additional sources for the Little Dal Formation, or at the very least unroofing of a progressively cooled metamorphic block in the source area. These samples are, however, distributed over a large geographical area and as a result it would be unwise to rule out variations in local point sources throughout the region.

These data also allow for reassessment of stratigraphic ages for the Mackenzie Mountains Supergroup. Detrital zircon U-Pb ages provide a crystallization age for the grain and may have been subject to several cycles of burial and exhumation since their formation. The $^{40}\text{Ar}/^{39}\text{Ar}$ geochronology, however, often yields information on the timing of the last tectonothermal episode experienced by the muscovite grain prior to deposition (Stuart, 2002) and as a result provides

a closer approximation to the true depositional age. The youngest age (992 ± 1 Ma) from the Tsezotene Formation is younger than the previous 1080 Ma detrital zircon age from the Upper Katherine Formation (Macdonald et al., 2012). While the boundary between the Katherine and Little Dal formations is erosional (Jefferson and Parrish, 1989), the youngest ages from samples JP009 and JP007 (lower Katherine and basal Little Dal formations, respectively) still provide a broad constraint on the timing of deposition of the Katherine Formation to between 965 Ma and 815 Ma. Similarly, the ca. 815 Ma muscovite $^{40}\text{Ar}/^{39}\text{Ar}$ age from the basal Little Dal formation from this study allows for better insight into the timing of deposition of the final unit in the Mackenzie Mountains Supergroup when compared with the ca. 780 Ma age associated with the top of the unit (Jefferson and Parrish, 1989). All of the $^{40}\text{Ar}/^{39}\text{Ar}$ ages are consistent with Grenvillian-aged tectonics in the source region, in accord with pre-existing hypotheses of sediment supply from the craton to the east (Young et al., 1979). While recent studies (Milidragovic et al., 2011) suggest that an overlooked connection between the Sibao Orogen of the South China Craton and the western margin of Laurentia may account for Grenvillian-age zircon grains in the Neoproterozoic strata, the evidence for a connection between the two paleocontinents is dubious (Macdonald et al., 2012).

Detrital zircon U-Pb studies on the Devonian–Mississippian strata of Northern Canada demonstrate that a majority of zircon grains are derived from Laurentia, to the east; however, an anomalous population of Lower Paleozoic and Neoproterozoic zircon ages are not consistent with any known magmatic event in Northern Canada and are thought to be derived from an exotic terrane to the north (Lemieux et al., 2011). Unlike the crystallization ages recorded in the U-Pb record, which may have undergone several depositional cycles since crystallization, the ages in the data of this study set reflect cooling in the most recent source terranes, forming the Imperial Formation, following uplift in the north and flushing of siliciclastic rocks into the Devonian basin (Hadlari et al., 2009).

Vertical tectonism as a consequence of the latest Devonian to Mississippian Ellesmerian Orogeny, a collisional event between Laurentia and an exotic terrane from the north (Gentzis and Goodarzi, 1993), is often invoked as the catalyst for deposition of the Imperial Formation (Williams, 1990; Hadlari et al., 2009). For the most part, the $^{40}\text{Ar}/^{39}\text{Ar}$ muscovite ages presented in this study are too old to be related to Ellesmerian-aged tectonism. Instead, the siliciclastic material must be sourced from an earlier tectonic event. One candidate may be the Romanzof Orogeny, a ca. 400 Ma event that caused shortening in northern Yukon and Alaska and was followed by a period of felsic plutonism between 375 Ma and 362 Ma (Colpron and Nelson, 2009). The 500–425 Ma ages cannot be resolved within the context of Early to Middle Devonian constraints of the Romanzof Orogeny. These ages may correspond with the 500–400 Ma ages associated with northern Appalachian–Caledonide

plutono-metamorphic complexes (Colpron and Nelson, 2009). Petrographically, the small grain size and abraded appearance of muscovite in the Imperial Formation may be indicative of minor reworking of the mineral following their initial erosion and transport. Thus, it is plausible that Ellesmerian tectonism reworked loose sediment shed during older tectonic events, depositing the material rapidly as the turbiditic Imperial Formation (Hadlari et al., 2009). It is interesting to note that the detrital muscovite $^{40}\text{Ar}/^{39}\text{Ar}$ ages in the present study bear a close resemblance to recent detrital zircon (U-Th)/He ages from Upper Devonian strata of the Franklinian basin of the Canadian Arctic (Anfinson et al., in press). When combined with detrital U-Pb ages, these data suggest that several arctic terranes experienced similar exhumational histories throughout the Silurian. Regardless of the final pathway, these ages support the hypothesis that tectonism related to the Late Silurian to Early Carboniferous convergence of a large terrane to northern Laurentia fueled deposition in the Devonian sea (Lane, 2007).

A tertiary age population observed in 10FNA192B01 and 10FNA138A02 (2.6–2.0 Ga) corresponds with detrital zircon age populations for the Imperial Formation. Zircon grains of these ages are common in the northern Cordillera and were potentially sourced from the Wopmay Orogen (Hadlari et al., 2009). The Neoproterozoic (675–575 Ma) population observed in sample 10FNA138B01 still requires an explanation, as the cooling ages significantly predate the timing of the Ellesmerian and Romanzof orogen events. Instead, these ages may be reflective of uplift in rift-related tectonic episodes. Additionally, they may be related to the enigmatic population of 700–500 Ma zircon grains reported in Lemieux et al. (2011). Independent of the source, it is likely that these sediments were eventually deposited in the same northern basin as the Romanzof-aged muscovite and reworked and redeposited during Devonian to Mississippian collision (Gentzis and Goodarzi, 1993).

SUMMARY

In summary, $^{40}\text{Ar}/^{39}\text{Ar}$ detrital muscovite ages for eight samples from the Mackenzie River corridor provide insight into the depositional and tectonic history for the region. The $^{40}\text{Ar}/^{39}\text{Ar}$ ages for strata from the Neoproterozoic Mackenzie Mountains Supergroup detail mostly Grenvillian-aged cooling in the source region and support the model of an eastern sediment source. In combination with pre-existing geochronological data, the youngest grains from the four Mackenzie Mountains Supergroup samples also serve to constrain the stratigraphic ages for the Mackenzie Mountains Supergroup to approximately 965–815 Ma for the Katherine Formation and 815–780 Ma for the Little Dal Formation, and a maximum age of ca. 1000 Ma for the Tsezotene Formation.

The $^{40}\text{Ar}/^{39}\text{Ar}$ ages from detrital muscovite in the four Devonian Imperial Formation samples yield ages corresponding to the ongoing collision of Laurentia and a northern landmass

throughout the Devonian. In particular, the most prevalent age population in all four samples corresponds with cooling that is similar in age to the Romanzof Orogeny: the detrital $^{40}\text{Ar}/^{39}\text{Ar}$ ages predate the Ellesmerian Orogeny, the event normally invoked as the driving tectonic force behind deposition of the Imperial Formation, leading to the interpretation that these sediments were shed into a northern basin prior to when previously interpreted.

ACKNOWLEDGMENTS

Funding for this project came from an NSERC CRD grant (to D.A. Schneider) in co-operation with ConocoPhillips Canada, Chevron, and the Geological Survey of Canada under the GEM initiative. R. MacNaughton and K. Fallas (GSC) are thanked for assistance in the field and discussions about the project, and M. Heizler (New Mexico Tech) is thanked for his help with the Ar-Ar data collection. D. Kellett is thanked for her critical review of the manuscript.

REFERENCES

- Adams, C.J. and Kelley, S., 1998. Provenance of Permian-Triassic and Ordovician metagraywacke terranes in New Zealand: evidence from $^{40}\text{Ar}/^{39}\text{Ar}$ of detrital micas; Geological Society of America Bulletin, v. 110, p. 422–432. [doi:10.1130/0016-7606\(1998\)110<0422:POPTAO>2.3.CO;2](https://doi.org/10.1130/0016-7606(1998)110<0422:POPTAO>2.3.CO;2)
- Aitken, J.D. and Long, D.G., 1978. Mackenzie tectonic arc – reflection of early basin configuration; Geology, v. 6, p. 626–629. [doi:10.1130/0091-7613\(1978\)6<626:MTAOEB>2.0.CO;2](https://doi.org/10.1130/0091-7613(1978)6<626:MTAOEB>2.0.CO;2)
- Anfinson, O.W., Leier, A.L., Dewing, K., Guest, B., Stockli, D.F., and Embry, A.F., in press: Insights into the Phanerozoic tectonic evolution of the northern Laurentian margin: detrital apatite and zircon (U-Th)/He ages from Devonian strata of the Franklinian Basin, Canadian Arctic Islands; Canadian Journal of Earth Sciences v. 50, no. 7, p. 761–768.
- Armstrong, R.L., Eisbacher, G.H., and Evans, P.D., 1982. Age and stratigraphic-tectonic significance of Proterozoic diabase sheets, Mackenzie Mountains, northwestern Canada; Canadian Journal of Earth Sciences, v. 19, p. 316–323. [doi:10.1139/e82-023](https://doi.org/10.1139/e82-023)
- Colpron, M. and Nelson, J.L., 2009. A Paleozoic Northwest Passage: incursion of Caledonian, Baltican and Siberian terranes into eastern Panthalassa, and the early evolution of the North American Cordillera; Geological Society of London, Special Publications, v. 318, p. 273–307. [doi:10.1144/SP318.10](https://doi.org/10.1144/SP318.10)
- Cook, D.G. and MacLean, B.C., 1999. The Imperial anticline, a fault-bend fold over a bedding-parallel thrust ramp, Northwest Territories, Canada; Journal of Structural Geology, v. 21, p. 215–228. [doi:10.1016/S0191-8141\(98\)00119-9](https://doi.org/10.1016/S0191-8141(98)00119-9)

- Gal, L.P. and Pyle, L.J., 2009. Chapter 5 – Upper Silurian–Lower Devonian strata (Delorme Group); *in* Regional Geoscience Studies and Petroleum Potential, Peel Plateau and Plain, Northwest Territories and Yukon: Project Volume, (ed.) L.J. Pyle and A.L. Jones; Northwest Territories Geoscience Office and Yukon Geological Survey; NWT Open File 2009-02 and YGS Open File 2009-25, p. 161–186.
- Gal, L.P., Pyle, L.J., Hadlari, T., and Allen, T.L., 2009. Chapter 6 – Lower to Upper Devonian strata, Arnica-Landry play, and Kee Scarp play; *in* Regional Geoscience Studies and Petroleum Potential, Peel Plateau and Plain, Northwest Territories and Yukon: Project Volume, (ed.) L.J. Pyle and A.L. Jones; Northwest Territories Geoscience Office and Yukon Geological Survey; NWT Open File 2009-02 and YGS Open File 2009-25, p. 187–289.
- Gentzis, T. and Goodarzi, F., 1993. Regional thermal maturity in Franklinian Mobile Belt, Melville Island, Arctic Canada; *Marine and Petroleum Geology*, v. 10, p. 215–230. [doi:10.1016/0264-8172\(93\)90105-2](https://doi.org/10.1016/0264-8172(93)90105-2)
- Hadlari, T., Tylosky, S.A., Lemieux, Y., Zantvoort, W.G., and Cantunean, O., 2009. Slope and submarine fan turbidite facies of the Upper Devonian Imperial Formation, Northern Mackenzie Mountains, NWT; *Bulletin of Canadian Petroleum Geology*, v. 57, p. 192–208. [doi:10.2113/gscpgbull.57.2.192](https://doi.org/10.2113/gscpgbull.57.2.192)
- Hadlari, T., Davis, W.J., Dewing, K., Heaman, L.M., Lemieux, Y., Ootes, L., Pratt, B.R., and Pyle, L.J., 2012. Two detrital zircon signatures for the Cambrian passive margin of northern Laurentia highlighted by new U-Pb results from northern Canada; *Geological Society of America Bulletin*, v. 124, p. 1155–1168. [doi:10.1130/B30530.1](https://doi.org/10.1130/B30530.1)
- Haines, P.W., Turner, S.P., Kelley, S.P., Wartho, J.A., and Sherlock, S.C., 2004. $^{40}\text{Ar}/^{39}\text{Ar}$ dating of detrital muscovite in provenance investigations: a case study from the Adelaide Rift Complex, South Australia; *Earth and Planetary Science Letters*, v. 227, p. 297–311. [doi:10.1016/j.epsl.2004.08.020](https://doi.org/10.1016/j.epsl.2004.08.020)
- Harrison, T.M. and Zeitler, P.K., 2005. Fundamentals of noble gas thermochronometry; *Reviews in Mineralogy and Geochemistry*, v. 58, p. 123–149. [doi:10.2138/rmg.2005.58.5](https://doi.org/10.2138/rmg.2005.58.5)
- Issler, D.R., Grist, A.M., and Statsiuk, L.D., 2005. Post-Early Devonian thermal constrains on hydrocarbon source rock maturation in the Keele Tectonic Zone, Tulita area, NWT, Canada, from multi-kinetic apatite fission track thermochronology, vitrinite reflectance and shale compaction; *Bulletin of Canadian Petroleum Geology*, v. 53, p. 405–431. [doi:10.2113/53.4.405](https://doi.org/10.2113/53.4.405)
- Jefferson, C.W. and Parrish, R.R., 1989. Late Proterozoic stratigraphy, U-Pb ages, and rift tectonics, Mackenzie Mountains, northwestern Canada; *Canadian Journal of Earth Sciences*, v. 26, p. 1784–1801. [doi:10.1139/e89-151](https://doi.org/10.1139/e89-151)
- Lane, L.S., 2007. Devonian-Carboniferous paleogeography and orogenesis, northern Yukon and adjacent Arctic Alaska; *Canadian Journal of Earth Sciences*, v. 44, no. 5, p. 679–694. [doi:10.1139/e06-131](https://doi.org/10.1139/e06-131)
- Lemieux, Y., Hadlari, T., and Simonetti, A., 2011. Detrital zircon geochronology and provenance of Devonian-Mississippian strata in the northern Canadian Cordillera miogeocline; *Canadian Journal of Earth Sciences*, v. 48, p. 515–541.
- Ludwig, K.R., 2008. User's manual for Isoplot version 3.70: a geochronological toolkit for Microsoft Excel; Berkley Geochronology Centre, Special Publication No. 4, 76 p.
- Macdonald, F.A., Halverson, G.P., Strauss, J.V., Smith, E.F., Cox, G., Sperling, E.A., and Roots, C.F., 2012. Early Neoproterozoic basin formation in Yukon, Canada: implications for the make-up and break-up of Rodinia; *Geoscience Canada*, v. 39, p. 77–99.
- MacLean, B.C. and Cook, D.G., 1999. Salt tectonism in the Fort Norman area, Northwest Territories, Canada; *Bulletin of Canadian Petroleum Geology*, v. 47, p. 104–135.
- MacNaughton, R.B., Fallas, K.M., and Zantvoort, W., 2008. Qualitative assessment of the Plateau Fault (Mackenzie Mountains, NWT) as a conceptual hydrocarbon play; Geological Survey of Canada, Open File 5831, 29 p. [doi:10.4095/225405](https://doi.org/10.4095/225405)
- Milidragovic, D., Thorkelson, D.J., Davis, W.J., Marshall, D.D., and Gibson, H.D., 2011. Evidence for late Mesoproterozoic tectonism in northern Yukon and the identification of a Grenville-age tectonothermal belt in western Laurentia; *Terra Nova*, v. 23, p. 307–313. [doi:10.1111/j.1365-3121.2011.01015.x](https://doi.org/10.1111/j.1365-3121.2011.01015.x)
- Mitchell, J.G. and Taka, A.S., 1984. Potassium and argon loss patterns in weathered micas: implications for detrital mineral studies, with particular reference to the Triassic Paleogeography of the British Isles; *Sedimentary Geology*, v. 39, p. 27–52. [doi:10.1016/0037-0738\(84\)90023-X](https://doi.org/10.1016/0037-0738(84)90023-X)
- Narbonne, G.M. and Aitken, J.D., 1995. Neoproterozoic of Mackenzie Mountain, northwestern Canada; *Precambrian Research*, v. 73, p. 101–121. [doi:10.1016/0301-9268\(94\)00073-Z](https://doi.org/10.1016/0301-9268(94)00073-Z)
- Patchett, P.J., Roth, M.A., Canale, B.S., de Freitas, T.A., Harrison, C.C., Embry, A.F., and Ross, G.M., 1999. Nd isotopes, geochemistry and constraints on sources of sediments in the Franklinian mobile belt, Arctic Canada; *Geological Society of America Bulletin*, v. 111, p. 578–589. [doi:10.1130/0016-7606\(1999\)111<0578:NIGACO>2.3.CO;2](https://doi.org/10.1130/0016-7606(1999)111<0578:NIGACO>2.3.CO;2)
- Pyle, L.J. and Gal, L.P., 2009a. Chapter 3 – Cambrian strata and basal Cambrian clastics play; *in* Regional Geoscience Studies and Petroleum Potential, Peel Plateau and Plain, Northwest Territories and Yukon: Project Volume, (ed.) L.J. Pyle and A.L. Jones; Northwest Territories Geoscience Office and Yukon Geological Survey; NWT Open File 2009-02 and YGS Open File 2009-25, p. 112–160.
- Pyle, L.J. and Gal, L.P., 2009b. Chapter 4 – Cambrian-Ordovician to Silurian strata and Lower Paleozoic platform (Ronning Group) play; *in* Regional Geoscience Studies and Petroleum Potential, Peel Plateau and Plain, Northwest Territories and Yukon: Project Volume, (ed.) L.J. Pyle and A.L. Jones; Northwest Territories Geoscience Office and Yukon Geological Survey; NWT Open File 2009-02 and YGS Open File 2009-25, p. 83–111.
- Reiners, P.W. and Brandon, M.T., 2006. Using thermochronology to understand orogenic erosion; *Annual Review of Earth and Planetary Sciences*, v. 34, p. 419–466. [doi:10.1146/annurev.earth.34.031405.125202](https://doi.org/10.1146/annurev.earth.34.031405.125202)

- Renne, P.R., Swisher, C.C., Deino, A.L., Karner, D.B., Owens, T.L., and DePaolo, D.J., 1998. Intercalibration of standards, absolute ages and uncertainties in $^{40}\text{Ar}/^{39}\text{Ar}$ dating; *Chemical Geology*, v. 145, p. 117–152. [doi:10.1016/S0009-2541\(97\)00159-9](https://doi.org/10.1016/S0009-2541(97)00159-9)
- Reynolds, P.H., Pe-Piper, G., and Piper, D.J., 2012. Detrital muscovite geochronology and the Cretaceous tectonics of the inner Scotian Shelf, southeastern Canada; *Canadian Journal of Earth Sciences*, v. 49, p. 1558–1566. [doi:10.1139/e2012-062](https://doi.org/10.1139/e2012-062)
- Steiger, R.H. and Jäger, E., 1977. Subcommittee on Geochronology: convention on the use of decay constants in geo- and cosmochronology; *Earth and Planetary Science Letters*, v. 36, p. 359–362.
- Stuart, F.M., 2002. The exhumational history of orogenic belts from $^{40}\text{Ar}/^{39}\text{Ar}$ ages of detrital micas; *Mineralogical Magazine*, v. 66, p. 121–135. [doi:10.1180/0026461026610017](https://doi.org/10.1180/0026461026610017)
- Turner, E.C. and Long, D.G., 2008. Basin architecture and syndepositional fault activity during deposition of the Neoproterozoic Mackenzie Mountain supergroup, Northwest Territories, Canada; *Canadian Journal of Earth Sciences*, v. 45, p. 1159–1184. [doi:10.1139/E08-062](https://doi.org/10.1139/E08-062)
- Williams, G.K., 1990. Tectonics and structure, Mackenzie Corridor, Northwest Territories; Geological Survey of Canada, Open File 2248, 26 p. [doi:10.4095/130901](https://doi.org/10.4095/130901)
- Young, G.M., Jefferson, C.W., Delaney, G.D., and Yeo, G.M., 1979. Middle and late Proterozoic evolution of the northern Canadian Cordillera and Shield; *Geology*, v. 7, p. 125–128. [doi:10.1130/0091-7613\(1979\)7<125:MALPEO>2.0.CO;2](https://doi.org/10.1130/0091-7613(1979)7<125:MALPEO>2.0.CO;2)

Geological Survey of Canada Project EGM003